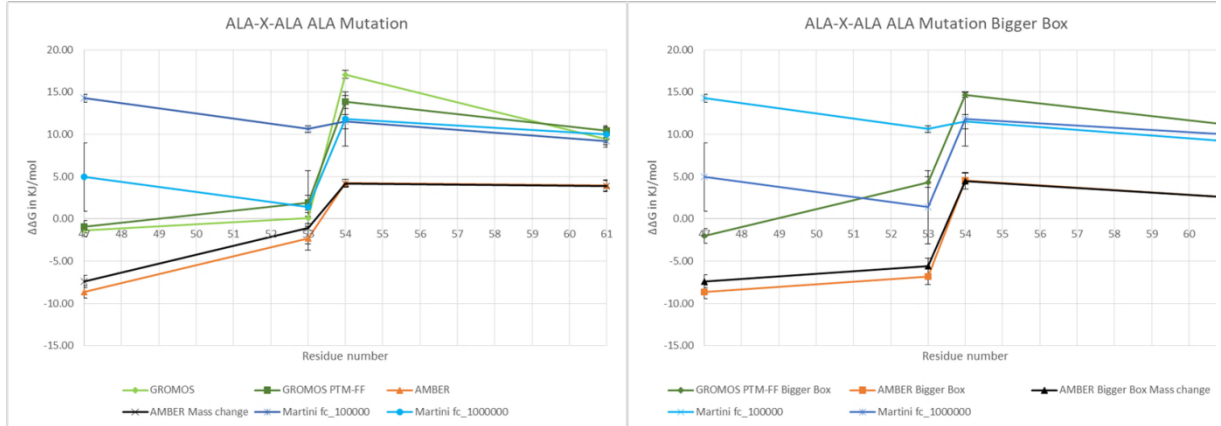
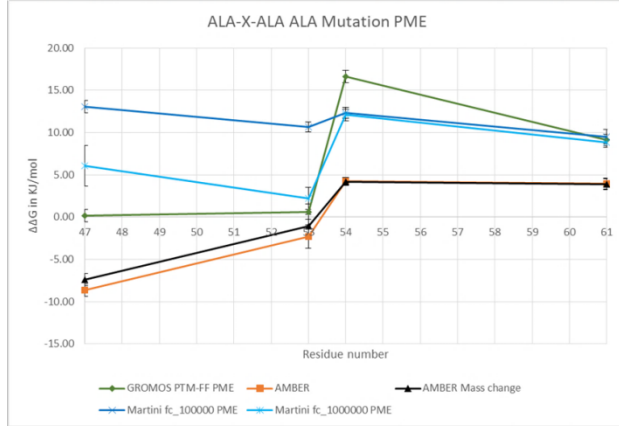


A

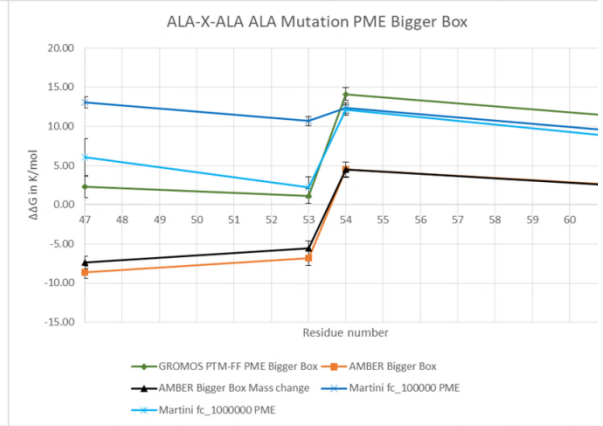


ALA-X-ALA ALA Mutation												
Residue number	GROMOS		GROMOS PTM-FF		AMBER		AMBER Mass change		Martini fc_100000		Martini fc_1000000	
	Value	st.dev	Value	st.dev	Value	st.dev	Value	st.dev	Value	st.dev	Value	st.dev
47	-1.37	0.68	-0.94	0.72	-8.66	0.72	-7.41	0.71	14.29	0.46	4.96	4.05
53	0.08	0.65	1.93	0.87	-2.33	1.39	-1.08	1.38	10.66	0.40	1.39	4.33
54	17.10	0.48	13.83	0.79	4.24	0.45	4.21	0.47	11.53	0.84	11.85	3.20
61	9.39	0.93	10.48	0.38	3.94	0.65	3.91	0.66	9.21	0.43	10.00	0.99

ALA-X-ALA ALA Mutation Bigger Box										
Residue number	GROMOS PTM-FF Bigger Box		AMBER Bigger Box		AMBER Bigger Box Mass change		Martini fc_100000		Martini fc_1000000	
	Value	st.dev	Value	st.dev	Value	st.dev	Value	st.dev	Value	st.dev
47	-2.02	0.88	-8.62	0.80	-7.37	0.78	14.29	0.46	4.96	
53	4.35	0.64	-6.80	0.93	-5.55	0.92	10.66	0.40	1.39	
54	14.67	0.30	4.51	0.96	4.48	0.97	11.53	0.84	11.85	
61	11.19	1.14	2.60	0.66	2.57	0.68	9.21	0.43	10.00	



ALA-X-ALA ALA Mutation PME										
Residue number	GROMOS PTM-FF PME		AMBER		AMBER Mass change		Martini fc_100000 PME		Martini fc_1000000 PME	
	Value	st.dev	Value	st.dev	Value	st.dev	Value	st.dev	Value	st.dev
47	0.15	0.72	-8.66	0.72	-7.41	0.71	13.05	0.73	6.07	2.38
53	0.62	0.91	-2.33	1.39	-1.08	1.38	10.68	0.58	2.23	1.32
54	16.62	0.72	4.24	0.45	4.21	0.47	12.33	0.66	12.09	0.68
61	9.11	0.66	3.94	0.65	3.91	0.66	9.51	0.83	8.84	0.61



ALA-X-ALA ALA Mutation Bigger Box PME										
Residue number	GROMOS PTM-FF PME Bigger Box		AMBER Bigger Box		AMBER Bigger Box Mass change		Martini fc_100000 PME		Martini fc_1000000 PME	
	Value	st.dev	Value	st.dev	Value	st.dev	Value	st.dev	Value	st.dev
47	2.28	1.39	-8.62	0.80	-7.37	0.78	13.05	0.73	6.07	
53	1.11	0.94	-6.80	0.93	-5.55	0.92	10.68	0.58	2.23	
54	14.12	0.83	4.51	0.96	4.48	0.97	12.33	0.66	12.09	
61	11.43	1.06	2.60	0.66	2.57	0.68	9.51	0.83	8.84	

B

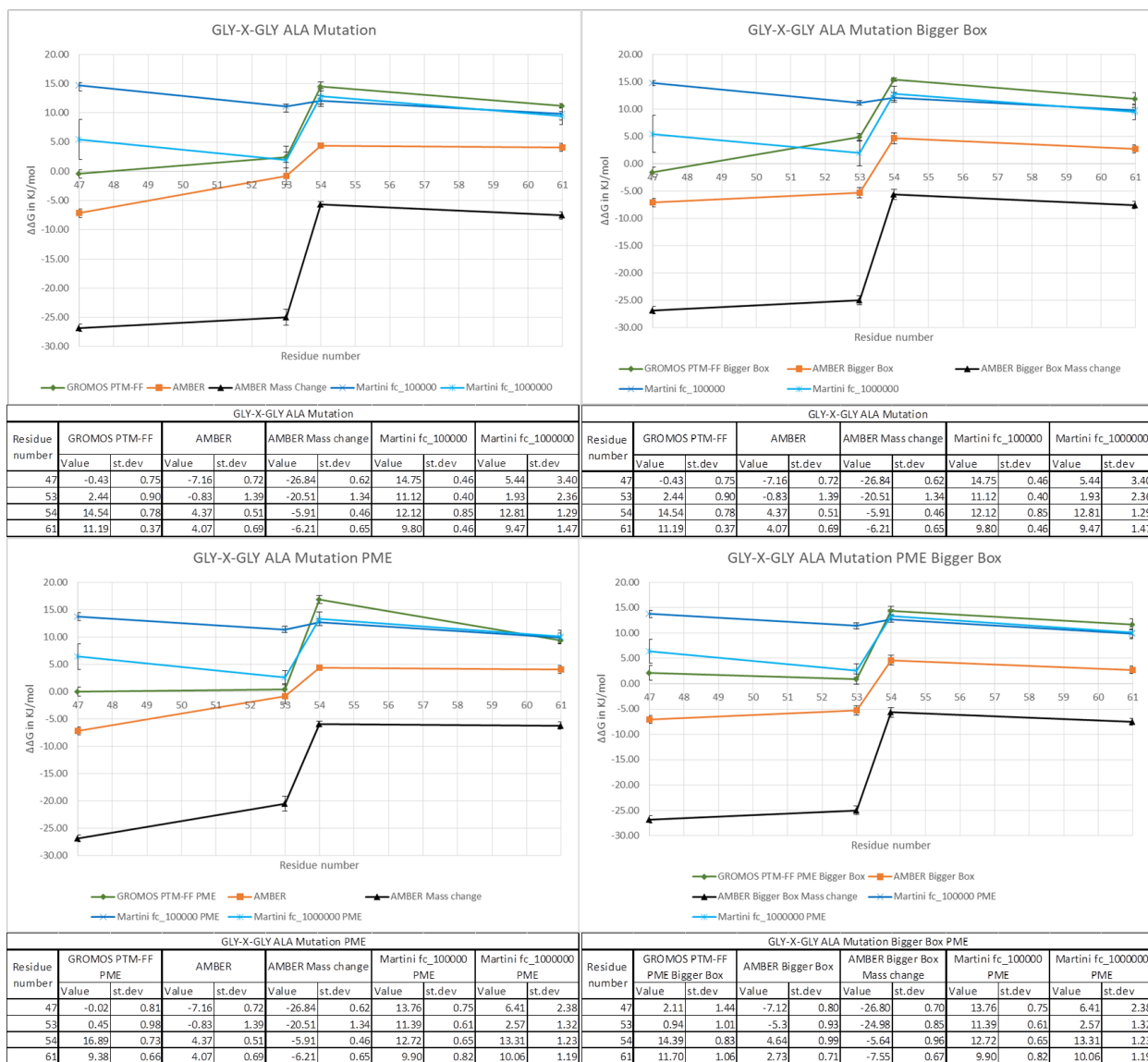
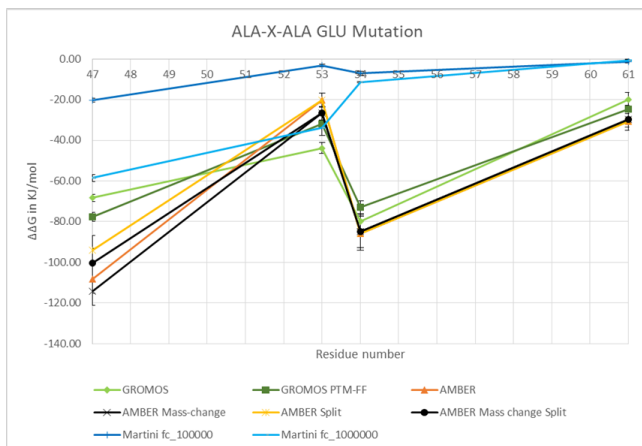


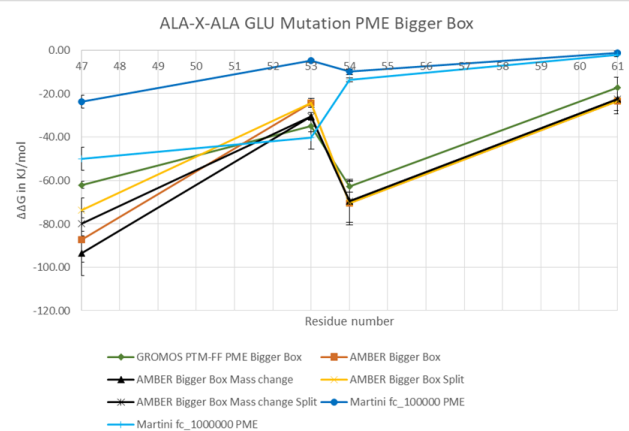
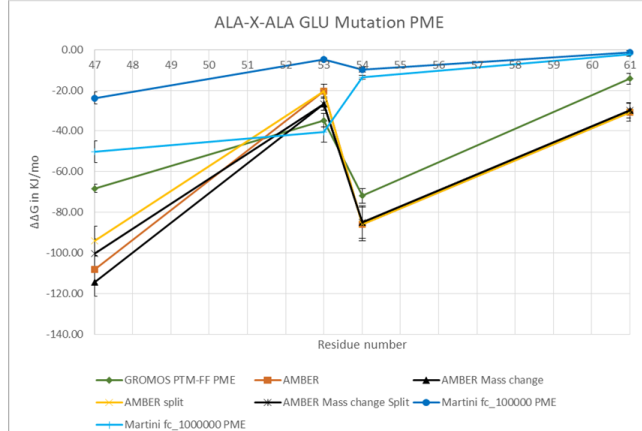
Figure S1: Mutations to alanine presented in a scatterplot graph. On the x-axis is the residue number of the residue being mutated, on the y-axis is the $\Delta\Delta G$ given in KJ/mol. GROMOS force field values are given in green, AMBER in orange and Martini in Blue. Given in black are the values for the AMBER force field calculated using tripeptides that shift mass, which may have reduced reliability. **A:** $\Delta\Delta G$ s calculated using ALA-X-ALA Tripeptides; **Top left:** the $\Delta\Delta G$ s of the simulations not using a bigger box size or PME. Graph indicated as simply GROMOS (given in light green) refers to values calculated using the force field without post translational modification. **Top right:** the $\Delta\Delta G$ s of the simulations using a bigger box size. **Bottom left:** the $\Delta\Delta G$ s of the simulations using PME. **Bottom right:** the $\Delta\Delta G$ s using both a bigger box size and PME. **B:** $\Delta\Delta G$ s calculated using GLY-X-GLY Tripeptides; **Top left:** the $\Delta\Delta G$ s of the simulations not using a bigger box size or PME. **Top right:** the $\Delta\Delta G$ s of the simulations using a bigger box size. **Bottom left:** the $\Delta\Delta G$ s of the simulations using PME. **Bottom right:** the $\Delta\Delta G$ s using both a bigger box size and PME.

A



Residue number	ALA-X-ALA GLU Mutation															
	GROMOS		GROMOS PTM-FF		AMBER		AMBER Mass change		AMBER Mass change Split		Martini fc_100000		Martini fc_1000000			
	Value	st.dev	Value	st.dev	Value	st.dev	Value	st.dev	Value	st.dev	Value	st.dev	Value	st.dev		
47	-8.35	1.77	-77.58	2.15	-108.14	6.99	-94.12	7.31	-114.39	6.91	-100.37	7.24	-20.29	0.95	-88.57	1.82
53	-43.80	2.63	-31.82	1.79	-20.36	3.46	-20.36	3.46	-26.61	3.31	-26.61	3.31	-3.27	0.62	-33.89	3.76
54	-79.90	3.67	-73.00	3.11	-85.74	8.41	-85.74	8.41	-84.82	8.08	-84.82	8.08	-6.99	1.00	-11.42	0.45
61	-19.89	3.39	-24.80	2.12	-30.77	4.42	-30.77	4.42	-29.85	3.75	-29.85	3.75	-1.25	0.71	-0.66	0.46

Residue number	ALA-X-ALA GLU Mutation Bigger Box													
	GROMOS PTM-FF Bigger Box		AMBER Bigger Box		AMBER Bigger Box Mass change Split		AMBER Bigger Box Mass change		AMBER Bigger Box Mass change Split		Martini fc_100000		Martini fc_1000000	
	Value	st.dev	Value	st.dev	Value	st.dev	Value	st.dev	Value	st.dev	Value	st.dev	Value	st.dev
47	-64.10	3.11	-87.44	10.23	-73.79	5.74	-93.69	10.18	-80.04	5.65	-20.29	0.95	-58.57	1.82
53	-39.28	1.99	-24.27	2.11	-24.27	2.11	-30.52	1.85	-30.52	1.85	-3.27	0.62	-33.89	3.76
54	-71.83	1.39	-70.38	10.07	-70.38	10.07	-69.46	9.80	-69.46	9.80	-6.99	1.00	-11.42	0.45
61	-22.22	3.92	-23.55	5.80	-23.55	5.80	-22.63	5.31	-22.63	5.31	-1.25	0.71	-0.66	0.46



Residue number	ALA-X-ALA GLU Mutation PME													
	GROMOS PTM-FF PME		AMBER		AMBER Split		AMBER Mass change		AMBER Mass change Split		Martini fc_100000 PME		Martini fc_1000000 PME	
	Value	st.dev	Value	st.dev	Value	st.dev	Value	st.dev	Value	st.dev	Value	st.dev	Value	st.dev
47	-68.19	2.12	-108.14	6.99	-94.12	7.31	-114.39	6.91	-100.37	7.24	-23.77	2.94	-50.12	5.31
53	-34.71	3.21	-20.36	3.46	-20.36	3.46	-26.61	3.31	-26.61	3.31	-4.72	0.66	-40.41	5.17
54	-71.87	3.66	-85.74	8.41	-85.74	8.41	-84.82	8.08	-84.82	8.08	-9.84	1.34	-13.60	0.95
61	-14.26	2.62	-30.77	4.42	-30.77	4.42	-29.85	3.75	-29.85	3.75	-1.21	0.76	-2.22	0.94

Residue number	ALA-X-ALA GLU Mutation Bigger Box PME													
	GROMOS PTM-FF PME Bigger Box		AMBER Bigger Box		AMBER Bigger Box Mass change Split		AMBER Bigger Box Mass change		AMBER Bigger Box Mass change Split		Martini fc_100000 PME		Martini fc_1000000 PME	
	Value	st.dev	Value	st.dev	Value	st.dev	Value	st.dev	Value	st.dev	Value	st.dev	Value	st.dev
47	-62.07	1.70	-87.44	10.23	-73.79	5.74	-93.69	10.18	-80.04	5.65	-23.77	2.95	-50.12	5.31
53	-34.97	2.73	-24.27	2.11	-24.27	2.11	-30.52	1.85	-30.52	1.85	-4.72	0.66	-40.41	5.17
54	-62.83	2.67	-70.38	10.07	-70.38	10.07	-69.46	9.80	-69.46	9.80	-8.84	1.34	-13.60	0.95
61	-17.22	4.61	-23.55	5.80	-23.55	5.80	-22.63	5.31	-22.63	5.31	-1.21	0.76	-2.22	0.94

B

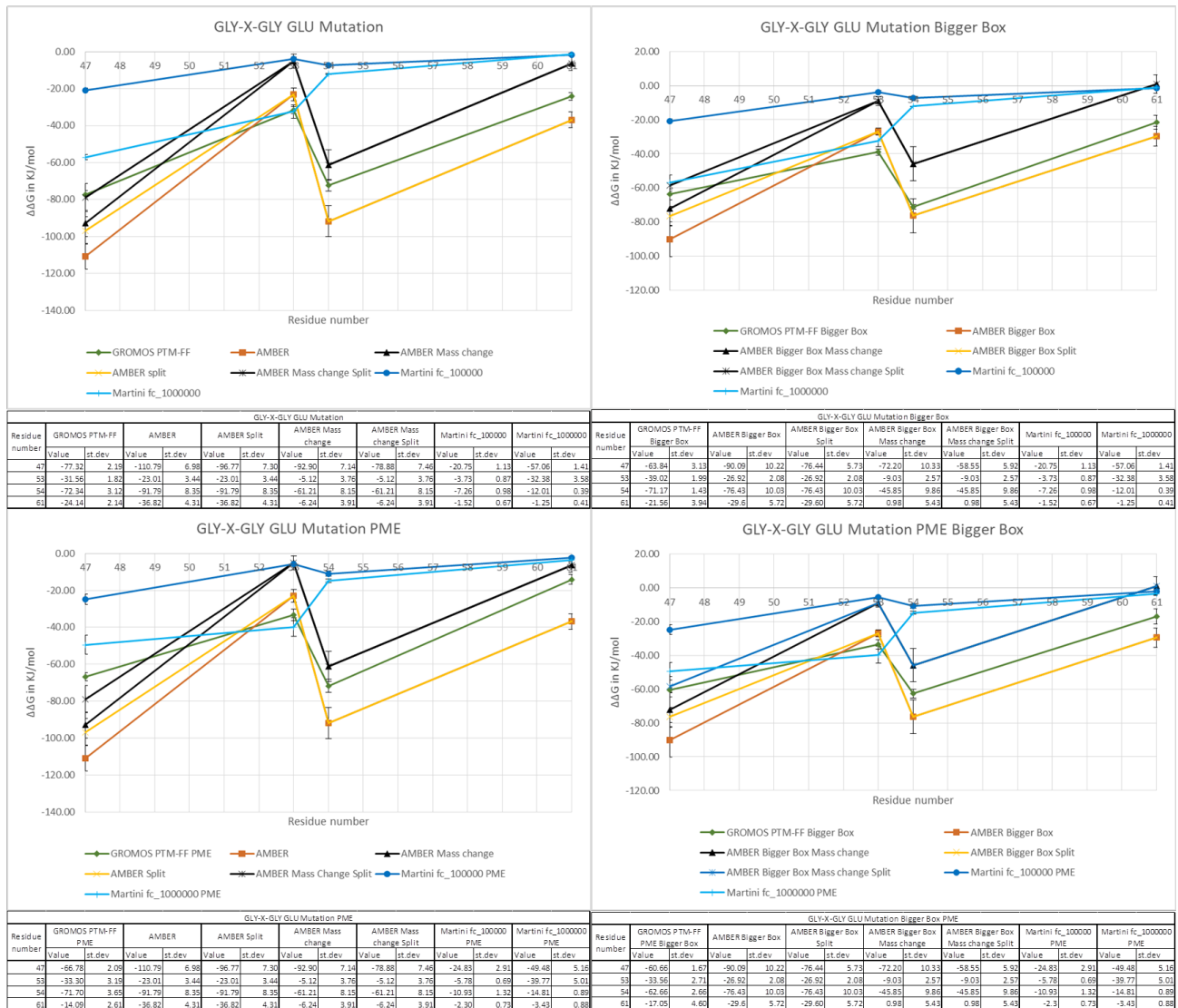
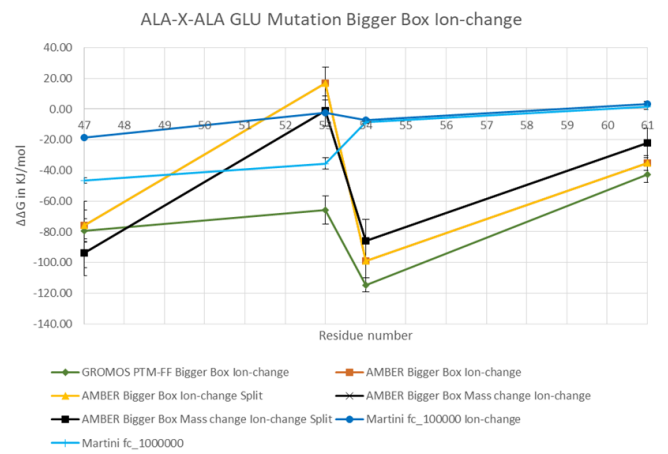
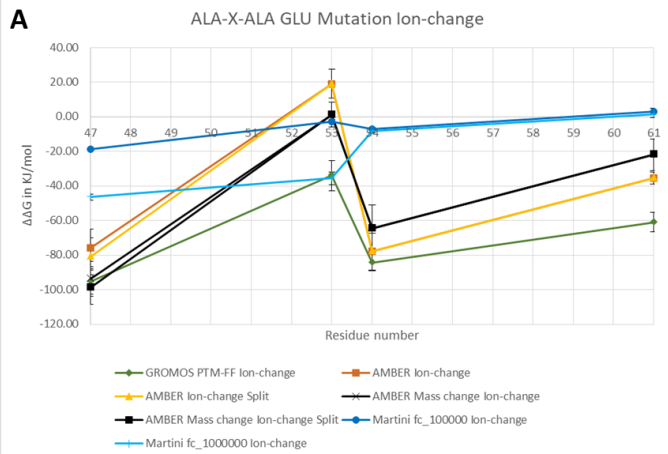
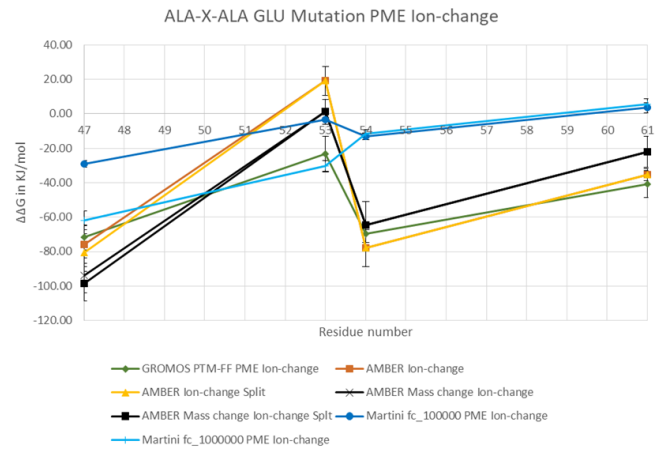
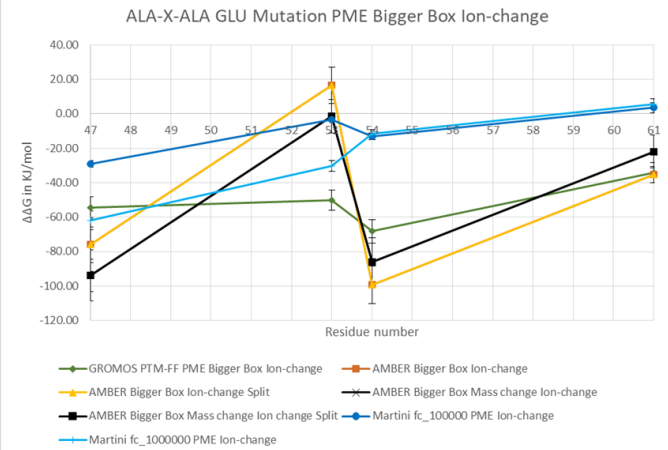


Figure S2: Mutations to Glutamate without the use of shifting ions presented in a scatterplot graph. On the x-axis is the residue number of the residue being mutated, on the y-axis is the $\Delta\Delta G$ given in kJ/mol. GROMOS force field values are given in green, AMBER in orange and Martini in blue. Given in black are the values for the AMBER force field calculated using tripeptides that shift mass, which may have reduced reliability. **A:** $\Delta\Delta G$ s calculated using ALA-X-ALA Tripeptides; **Top left:** the $\Delta\Delta G$ s of the simulations not using a bigger box size, PME or shifting ions. Graph indicated as simply GROMOS (given in light green) refers to values calculated using the force field without post translational modification. **Top right:** the $\Delta\Delta G$ s of the simulations using a bigger box size. **Bottom left:** the $\Delta\Delta G$ s of the simulations using PME. **Bottom right:** the $\Delta\Delta G$ s using both a bigger box size and PME. **B:** $\Delta\Delta G$ s calculated using GLY-X-GLY Tripeptides; **Top left:** the $\Delta\Delta G$ s of the simulations not using a bigger box size, PME or shifting ions. **Top right:** the $\Delta\Delta G$ s of the simulations using a bigger box size. **Bottom left:** the $\Delta\Delta G$ s of the simulations using PME. **Bottom right:** the $\Delta\Delta G$ s using both a bigger box size and PME.



Residue number	ALA-X-ALA GLU Mutation Ion-change													
	GROMOS PTM-FF Ion-change		AMBER Ion-change		AMBER Ion-change Split		AMBER Mass change Ion-change		AMBER Mass change Ion-change Split		Martini fc_100000 Ion-change		Martini fc_1000000 Ion-change	
	Value	st dev	Value	st dev	Value	st dev	Value	st dev	Value	st dev	Value	st dev	Value	st dev
47	-95.29	7.38	-75.87	10.86	-80.71	10.87	-93.81	10.02	-98.65	9.93	-18.69	1.15	-46.49	1.76
53	-84.08	8.67	19.09	8.48	19.09	8.48	1.15	7.24	1.15	7.24	-2.64	0.93	-35.63	3.65
54	-84.25	4.95	-77.98	10.77	-77.98	10.77	-64.58	13.65	-64.58	13.65	-7.12	0.84	-8.41	1.05
61	-60.91	5.48	-35.41	3.62	-35.41	3.62	-22.01	9.05	-22.01	9.05	3.11	1.71	1.27	1.75

Residue number	ALA-X-ALA GLU Mutation Bigger Box Ion-change													
	GROMOS PTM-FF Bigger Box Ion-change		AMBER Bigger Box Ion-change		AMBER Bigger Box Ion-change Split		AMBER Bigger Box Mass change Ion-change		AMBER Bigger Box Mass change Ion-change Split		Martini fc_100000 Bigger Box Ion-change		Martini fc_1000000 Bigger Box Ion-change	
	Value	st dev	Value	st dev	Value	st dev	Value	st dev	Value	st dev	Value	st dev	Value	st dev
47	-79.34	7.74	-75.87	15.56	-76.03	10.37	-93.81	14.92	-93.97	9.38	-18.69	1.15	-46.49	1.76
53	-65.86	9.27	16.55	10.68	16.55	10.68	-1.39	9.72	-1.39	9.72	-3.64	0.93	-35.63	3.65
54	-114.59	4.53	-99.25	10.91	-99.25	10.91	-85.85	13.70	-85.85	13.70	-7.12	0.84	-8.41	1.05
61	-42.66	5.19	-35.43	4.77	-35.43	4.77	-22.03	9.56	-22.03	9.56	3.11	1.71	1.27	1.75



Residue number	ALA-X-ALA GLU Mutation PME Ion-change													
	GROMOS PTM-FF PME Ion-change		AMBER Ion-change		AMBER Ion-change Split		AMBER Mass change Ion-change		AMBER Mass change Ion-change Split		Martini fc_100000 PME Ion-change		Martini fc_1000000 PME Ion-change	
	Value	st dev	Value	st dev	Value	st dev	Value	st dev	Value	st dev	Value	st dev	Value	st dev
47	-71.65	7.24	-75.87	10.86	-80.71	10.87	-93.81	10.02	-98.65	9.93	-25.17	1.84	-61.95	5.36
53	-23.37	10.30	19.09	8.48	19.09	8.48	1.15	7.24	1.15	7.24	-3.24	1.14	-30.35	3.13
54	-69.59	5.38	-77.98	10.77	-77.98	10.77	-64.58	13.65	-64.58	13.65	-13.04	1.87	-11.56	2.15
61	-40.96	7.85	-35.41	3.62	-35.41	3.62	-22.01	9.05	-22.01	9.05	3.50	3.06	5.63	2.96

Residue number	ALA-X-ALA GLU Mutation Bigger Box PME Ion-change													
	GROMOS PTM-FF PME Bigger Box Ion-change		AMBER Bigger Box Ion-change		AMBER Bigger Box Ion-change Split		AMBER Bigger Box Mass change Ion-change		AMBER Bigger Box Mass change Ion-change Split		Martini fc_100000 PME Ion-change		Martini fc_1000000 PME Ion-change	
	Value	st dev	Value	st dev	Value	st dev	Value	st dev	Value	st dev	Value	st dev	Value	st dev
47	-54.58	6.44	-75.87	15.56	-76.03	10.37	-93.81	14.92	-93.97	9.38	-25.17	1.84	-61.95	5.36
53	-50.11	5.88	16.55	10.68	16.55	10.68	-1.39	9.72	-1.39	9.72	-3.24	1.14	-30.35	3.13
54	-68.16	6.83	-99.25	10.91	-99.25	10.91	-85.85	13.70	-85.85	13.70	-13.04	1.87	-11.56	2.15
61	-34.14	6.00	-35.43	4.77	-35.43	4.77	-22.03	9.56	-22.03	9.56	3.50	3.06	5.63	2.96

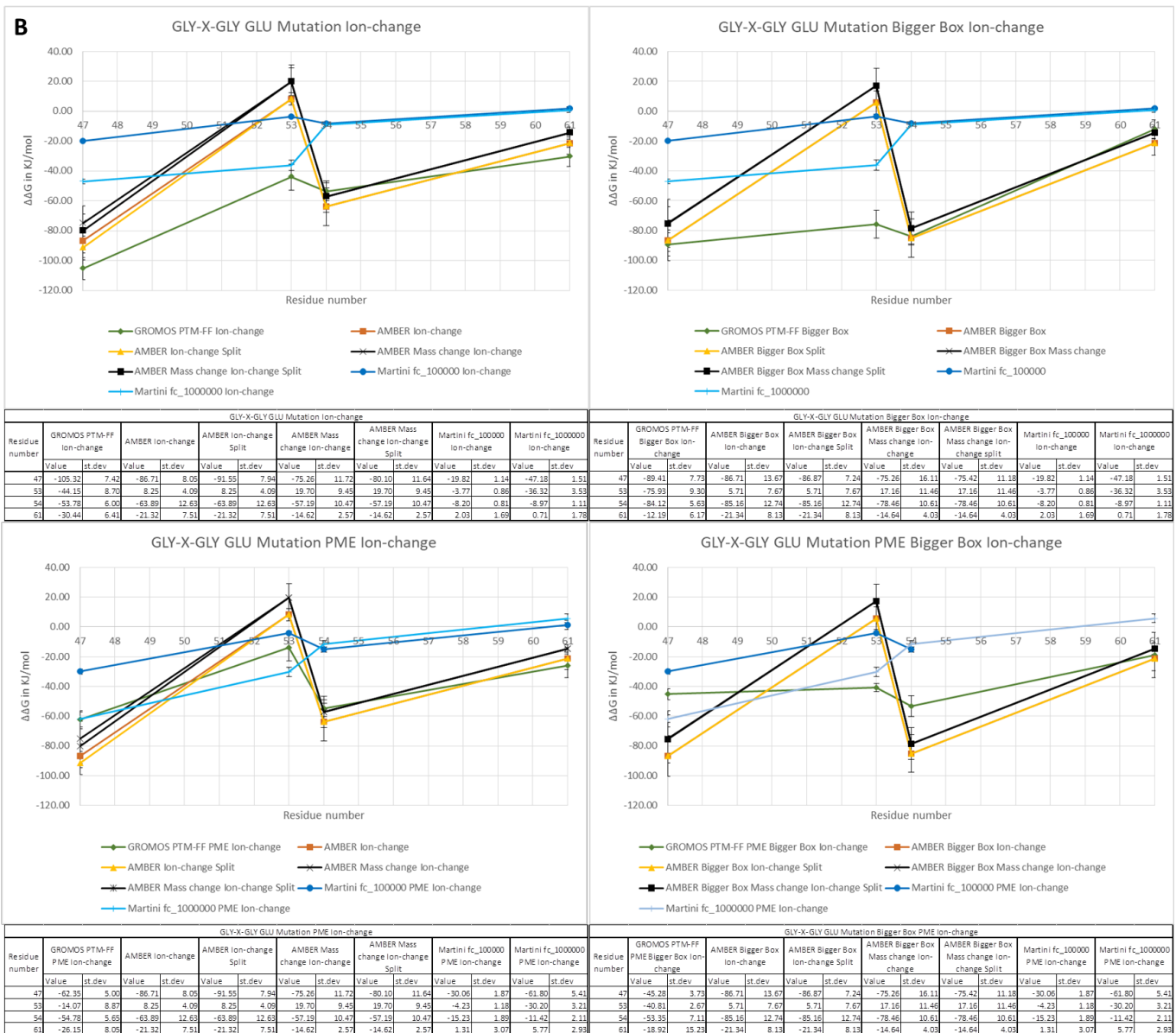
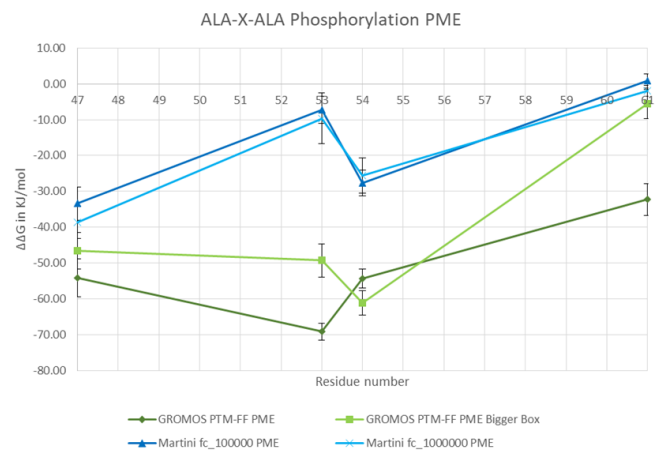
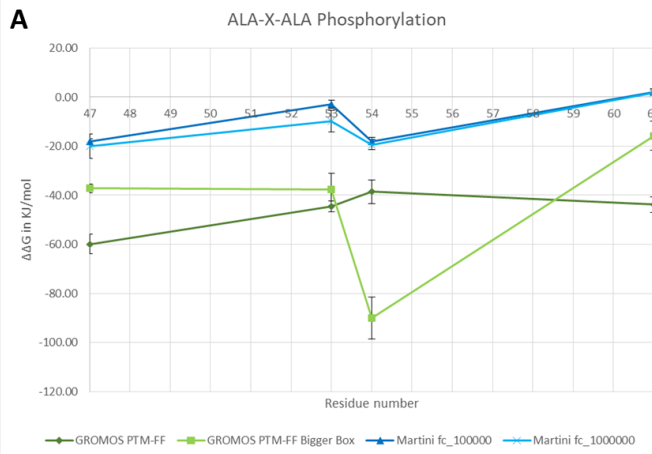
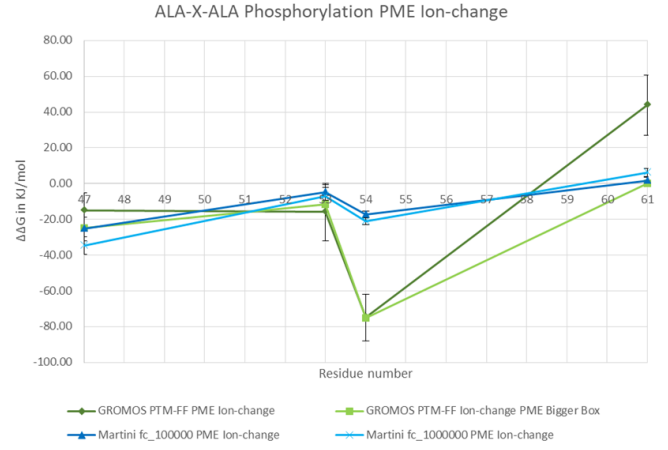
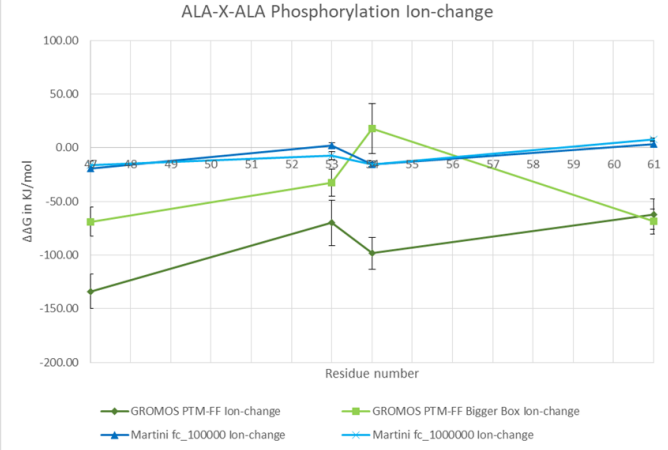


Figure S3: Mutations to Glutamate with the use of shifting ions presented in a scatterplot graph. On the x-axis is the residue number of the residue being mutated, on the y-axis is the $\Delta\Delta G$ given in KJ/mol. GROMOS force field values are given in green, AMBER in orange and Martini in Blue. Given in black are the values for the AMBER force field calculated using tripeptides that shift mass, which may have reduced reliability. **A:** $\Delta\Delta G$ s calculated using ALA-X-ALA Tripeptides; **Top left:** the $\Delta\Delta G$ s of the simulations using only shifting ions. **Top right:** the $\Delta\Delta G$ s of the simulations using a bigger box size and shifting ions. **Bottom left:** the $\Delta\Delta G$ s of the simulations using PME and shifting ions. **Bottom right:** the $\Delta\Delta G$ s using both a bigger box size, PME and shifting ions. **B:** $\Delta\Delta G$ s calculated using GLY-X-GLY Tripeptides; **Top left:** the $\Delta\Delta G$ s of the simulations using only shifting ions. **Top right:** the $\Delta\Delta G$ s of the simulations using a bigger box size and shifting ions. **Bottom left:** the $\Delta\Delta G$ s of the simulations using PME and shifting ions. **Bottom right:** the $\Delta\Delta G$ s using both a bigger box size, PME and shifting ions.



Residue number	ALA-X-ALA Phosphorylation							
	GROMOS PTM-FF		GROMOS PTM-FF Bigger Box		Martini fc_100000		Martini fc_1000000	
	Value	st.dev	Value	st.dev	Value	st.dev	Value	st.dev
47	-59.86	4.01	-37.20	1.83	-18.21	1.32	-20.00	4.85
53	-44.49	2.27	-37.68	6.70	-2.99	1.62	-9.80	4.45
54	-38.60	4.74	-90.02	8.49	-17.97	1.39	-19.42	2.09
61	-43.75	3.16	-15.78	5.94	2.08	1.29	1.82	1.10

Residue number	ALA-X-ALA Phosphorylation PME							
	GROMOS PTM-FF PME		GROMOS PTM-FF PME Bigger Box		Martini fc_100000 PME		Martini fc_1000000 PME	
	Value	st.dev	Value	st.dev	Value	st.dev	Value	st.dev
47	-54.09	5.30	-46.57	5.14	-33.42	4.70	-38.69	4.52
53	-69.18	2.35	-49.31	4.58	-7.26	3.74	-9.62	7.08
54	-54.28	2.65	-61.16	3.38	-27.71	3.58	-25.61	4.88
61	-32.24	4.44	-5.64	3.99	0.83	2.01	-1.96	1.49



Residue number	ALA-X-ALA Phosphorylation Ion-change							
	GROMOS PTM-FF Ion-change		GROMOS PTM-FF Bigger Box Ion-change		Martini fc_100000 Ion-change		Martini fc_1000000 Ion-change	
	Value	st.dev	Value	st.dev	Value	st.dev	Value	st.dev
47	-133.78	15.97	-68.81	13.39	-19.07	0.97	-15.97	3.70
53	-69.82	21.18	-32.28	12.58	2.19	2.44	-7.09	3.78
54	-98.26	14.84	17.91	23.08	-15.36	1.71	-15.18	2.97
61	-61.93	14.37	-68.56	11.59	3.67	1.96	7.74	1.48

Residue number	ALA-X-ALA Phosphorylation PME Ion-change							
	GROMOS PTM-FF PME Ion-change		GROMOS PTM-FF PME Bigger Box Ion-change		Martini fc_100000 PME Ion-change		Martini fc_1000000 PME Ion-change	
	Value	st.dev	Value	st.dev	Value	st.dev	Value	st.dev
47	-14.99	9.75	-24.74	10.33	-25.34	6.68	-34.65	4.85
53	-15.84	16.04	-11.69	9.43	-4.93	4.28	-7.01	4.80
54	-74.88	13.02	-75.31	16.98	-17.20	1.73	-21.07	1.96
61	43.87	16.93	0.29	16.66	1.72	1.77	6.30	2.32

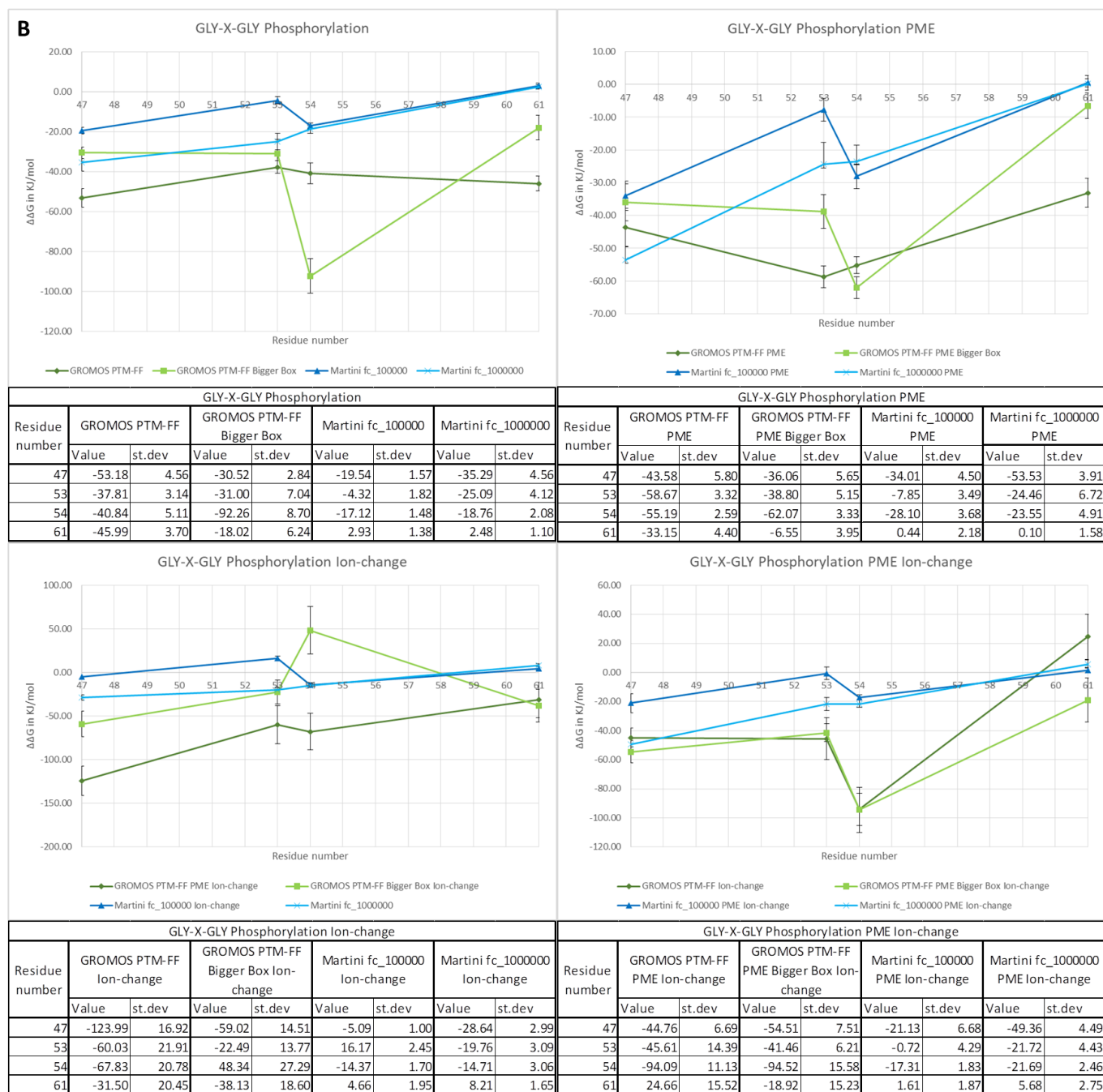


Figure S4: Phosphorylation presented in a scatterplot graph. On the x-axis is the residue number of the residue being mutated, on the y-axis is the $\Delta\Delta G$ given in KJ/mol. GROMOS force field values are given in green and Martini in Blue. **A:** $\Delta\Delta G$ s calculated using ALA-X-ALA Tripeptides; **Top left:** the $\Delta\Delta G$ s of the simulations not using PME or shifting ions, both with and without the use of a bigger box size. **Top right:** the $\Delta\Delta G$ s of the simulations using PME, both with and without the use of a bigger box size. **Bottom left:** the $\Delta\Delta G$ s of the simulations using shifting ions, both with and without the use of a bigger box size. **Bottom right:** the $\Delta\Delta G$ s of the simulations using PME and shifting ions, both with and without the use of a bigger box size. **B:** $\Delta\Delta G$ s calculated using GLY-X-GLY Tripeptides; **Top left:** the $\Delta\Delta G$ s of the simulations not using PME or shifting ions, both with and without the use of a bigger box size. **Top right:** the $\Delta\Delta G$ s of the simulations using PME, both with and without the use of a bigger box size. **Bottom left:** the $\Delta\Delta G$ s of the simulations using shifting ions, both with and without the use of a bigger box size. **Bottom right:** the $\Delta\Delta G$ s of the simulations using PME and shifting ions, both with and without the use of a bigger box size.

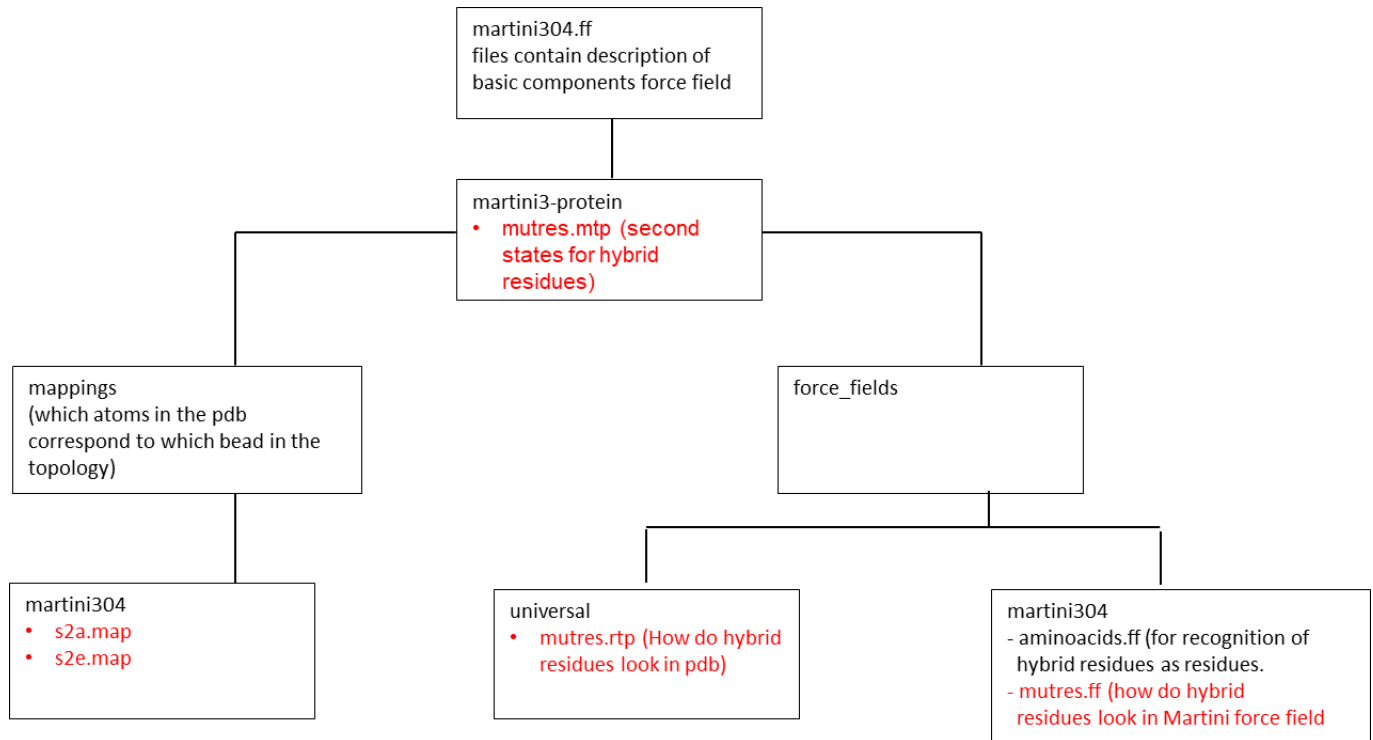


Figure S5: Flowchart visualizing the structure of the Martini 3.0.4 force field, files given in red are new for the martini-pmx version. To add a new hybrid residue to the force field the following components need to be added to the following locations or files. universal/mutres.rtp needs to have the appearance of the hybrid residue in the pdb file. martini304/mutres.ff needs to have the definition of the hybrid residue for the topologies. martini304/aminoacids.ff needs to have the names of the new hybrid residues added to list of residues. mappings\martini304 needs to have a file which describes which atom of the residue in the pdb file maps to which bead of the same residue in the Martini3 topology. mutres.mtp needs to have the topology of the hybrid residue with the second states present.

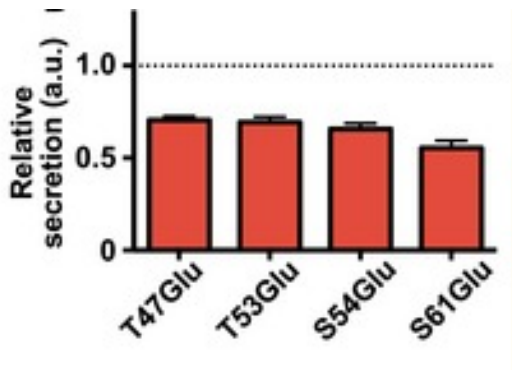


Figure S6: bar graph from *Malmersjö et al.*¹ (specifically figure 4B) visualizing the results of the effect of mutating the key residues to glutamate. On the y-axis is the amount of mast cell secretion relative to the values of wild type VAMP8, on the x-axis the mutation.

Mutation	ALA-X-ALA				GLY-X-GLY			
	Without Cut-off		With Cut-off		Without Cut-off		With Cut-off	
	Val	st.dev	Val	st.dev	Val	st.dev	Val	st.dev
S54pS GROMOS PTM-FF Ion-change Bigger Box	17.91	23.08	54.32	12.40	48.34	27.29	84.75	19.12
S61pS GROMOS PTM-FF Ion-change PME	43.87	16.93	43.38	11.51	24.66	15.52	24.17	9.32
T53pT AMBER Ion- change	19.09	8.48	22.44	8.71	8.25	4.09	11.60	4.56
T53pT AMBER Bigger Box Ion- change	16.55	10.68	25.19	9.81	5.71	7.67	14.35	6.42
T53pT Martini fc_100000 Ion- change	2.19	2.44	-4.51	2.80	16.17	2.45	9.47	2.81

Figure S7: Table showing the values of the deviant positive values before for the mutations to glutamate and for phosphorylation. Both ALA-X-ALA and GLY-X-GLY values were shown, both values before and after cutting of the first 2 ns of the simulations time are shown.

In depth description of the simulation of the mutations to glutamate

Mutating the key residues (T47, T53, S54 and S61) to glutamate (figure S2, figure S3) generally resulted in a negative $\Delta\Delta G$ which indicates that the mutation increased the free energy of folding and thus making folding more unfavorable.

In almost all cases the $\Delta\Delta G$ of T47E was lower than that of T53E which is higher than that of S54E, the $\Delta\Delta G$ of S54E is lower than that of S61E. The exception to this rule being fc_1000000 simulations where T53E has a lower value than S54E but the rest of the pattern is the same. T47E had a more negative $\Delta\Delta G$ than S54E for the AMBER force field unless the combination of a bigger box size and shifting ions (figure S3) are used, in which case the opposite is true. For the GROMOS force field T47E had a more negative $\Delta\Delta G$ than S54E when shifting ions without a bigger box size are used (figure S3), but a less negative $\Delta\Delta G$ under all other conditions.

In the Martini fc_1000000 simulations the T47E and T53E mutations had at first instance large standard deviations ($\sim 30-40$ kJ/mol), those turned out to be caused by the fact that the chosen length for the equilibration run had been too short for this type of mutation in the Martini force field as both tripeptides as SNAREs fluctuated heavily in the first $\sim 1000-2000$ ps. Cutting the first 2000 ps off solved this issue and significantly reduced the standard deviation to be ≤ 5.41 kJ/mol.

Increasing the box size (figure S2) did significantly alter the values of the $\Delta\Delta G$ and the standard deviation. For the GROMOS force field the average values increased at most ~ 15 kJ/mol (T47E) but for S54E and S61E the increase was less than 2.5 kJ/mol, in case of T53E an decrease of ~ 8 kJ/mol occurred. The effect on the AMBER force field was stronger increasing the average values by as much as 20 kJ/mol, this does reduce the total difference in $\Delta\Delta G$ between the force fields. The increase in the AMBER force field is however lower for GLY-X-GLY, which means the reduction of the differences between GROMOS and AMBER is also less strong. For the rest the effects were the same as with ALA-X-ALA. For both ALA-X-ALA and GLY-X-GLY increasing the box size caused an increase in

standard deviation for AMBER for T47E and S54E but an decrease in standard deviation for T53E and S61E.

The usage of PME (figure S2) for GROMOS and Martini force fields did significantly alter the values for GROMOS and Martini $fc_{1000000}$ (not for AMBER as AMBER can only use PME electrostatics). GROMOS is affected in the same manner as when the box size is increased except the increase with S61E is higher (~ 10 kJ/mol vs 2.5 kJ/mol) and the decrease with T53E is less strong (~ 3 kJ/mol vs ~ 8 kJ/mol). Thus the differences between the GROMOS and AMBER force fields became bigger instead of smaller. For the Martini fc_{100000} all values became more negative and thus closer to the values of both the GROMOS and AMBER force fields, but the shifts were all within or close to 2.5 kJ/mol of the values without PME. For Martini $fc_{1000000}$ the shift was in the same direction but stronger with the shift of T47E and T53E being ~ 8 kJ/mol, while for S54E and S61E remained within 2.5 kJ/mol of the values without PME. The effect is the same for GLY-X-GLY.

When using both a bigger box size and PME (figure S2) the $\Delta\Delta G$ values of the GROMOS force field were less negative than with only bigger box size, but the values for AMBER are the same (AMBER can only use PME). This means that differences between the GROMOS and AMBER force fields are bigger than when only the bigger box size is used, but the differences are however less severe than under conditions without alterations or when only PME is used.

Using ions that shift state (figure S3) had some interesting effects on the simulations. First to note is for the AMBER and GROMOS force fields both the ΔG_1 and ΔG_4 became ~ 1.5 - 2.0 as big as before. For the GROMOS force field all the $\Delta\Delta G$ s became more negative, T53E by as little as ~ 2.5 kJ/mol, S61E by as much as 40 kJ/mol. For the AMBER force field almost all the $\Delta\Delta G$ s became less negative, only S61E became more negative by ~ 5 kJ/mol, the rest all became less negative. T53E became positive at a value of 19.09 kJ/mol while the rest remained negative. For the Martini force field the changes were less severe; with the fc_{100000} the $\Delta\Delta G$ s remained within or close to 2.5 kJ/mol of the values under conditions without alterations, with the $fc_{1000000}$ variant only T47E had a change of more than 10 kJ/mol (in the positive direction) all other changes were within or close to 2.5 kJ/mol of the values under conditions without alterations. It must be noted however that for both fc_{100000} and $fc_{1000000}$ variants S61E went from a negative to a positive value but both before and after shift were within 2.5 kJ/mol of zero.

For GROMOS combining shifting ions and a bigger box size (figure S3) makes T47E and S61E less negative by ~ 15 - 20 kJ/mol while T53E and S54E become more negative by ~ 30 kJ/mol (in comparison to only using shifting ions). For AMBER T53E became more positive by ~ 20 kJ/mol, all other mutations remained within 2.5 kJ/mol of their values when only shifting ions were used, the one exception being the split T47E simulation (see below).

For GROMOS combining the use shifting ions and PME (figure S3) makes all $\Delta\Delta G$ s less negative by ~ 15 - 30 kJ/mol in comparison to using only shifting ions. The values of AMBER did not change as AMBER can only use PME. With the exception of T53E all $\Delta\Delta G$ were within ~ 5 - 7 kJ/mol of the AMBER force field without split simulation. For the Martini force field fc_{100000} variant T47E and S54E became more negative by ~ 10 kJ/mol, T53E and S61E remained within 2.5 kJ/mol of the value when only shifting ions are used. For Martini $fc_{1000000}$ the shift was similar but different; T47E became more negative by ~ 15 kJ/mol instead of ~ 10 , T53E and S61E became more negative by ~ 5 and ~ 4

kJ/mol respectively instead of remaining within or close to 2.5 kJ/mol, for S54E the shift is the same however.

For GROMOS using the combination of shifting ion, a bigger box size and PME (figure S3) made T47E less negative by ~20 kJ/mol in comparison to only using shifting ion and PME, T53E became more negative by ~30 kJ/mol, S54E remained within 2.5 kJ/mol and S61E became less negative by ~5 kJ/mol. The differences with the AMBER force field are 20 kJ/mol or larger, the only exception being S61E where the difference is smaller than 2.5 kJ/mol, this means that in general the differences have become larger than when using only shifting ions and PME, and also bigger than when only shifting ions and a bigger box size were used.

For GLY-X-GLY using shifting ions (figure S3) had some different effects on the GROMOS force field than with ALA-X-ALA; the $\Delta\Delta G$ of T47E became more negative by ~30 kJ/mol instead of by ~20 kJ/mol, the one of T53E became more negative by ~12 kJ/mol instead of by ~2 kJ/mol, the one of S54E became less negative by ~30 kJ/mol instead of becoming more negative by about 10 kJ/mol and the one of S61E stayed within 2.5 kJ/mol of the value prior to using shifting ions instead of increasing by ~40 kJ/mol. This also means that when shifting ions are used the $\Delta\Delta G$ s of the GROMOS force fields are no longer within or close to 2.5 kJ/mol of their ALA-X-ALA counterparts. For AMBER T47E and T53E were effected in the same manner as with ALA-X-ALA becoming positive at 8.25 kJ/mol, However S54E became less negative by ~30 kJ/mol instead of by ~10 kJ/mol and S61E became less negative by ~15 kJ/mol instead of 5 kJ/mol.

The shifts induced by the use of a bigger box size in combination with shifting ions (figure S3) in comparison to when only shifting ions are used are the same as for ALA-X-ALA. When using PME in addition to shifting ions (figure S3) the shifts in comparison to when only shifting were used are different from ALA-X-ALA however. For the GROMOS force field; T47E, T53E and S61E became less negative by ~40, ~30 and ~4 kJ/mol respectively instead of ~25, ~10 and ~20 kJ/mol, S54E remains within 2.5 kJ/mol of when only shifting ions are used instead of becoming less negative by ~15 kJ/mol. When using shifting ions, a bigger box size and PME (figure S3) the shift in comparison to when only shifting ions and PME are used is the same as for ALA-X-ALA. For the Martini force field using shifting ion induced the same changes as for ALA-X-ALA for both fc_{100000} and $fc_{1000000}$. Using PME in combination with shifting ion induced the same changes in comparison to only using shifting ion as with ALA-X-ALA.

Unlike with ALA-X-ALA it is less clear under which conditions the differences are the smallest between GROMOS and AMBER force fields. As with ALA-X-ALA the combination of PME and shifting ions is a promising candidate but there are some differences; T47E has ~4 (ALA-X-ALA) vs ~24 kJ/mol (GLY-X-GLY), T53E has ~42 (ALA-X-ALA) vs ~24 kJ/mol (GLY-X-GLY), with S54E and S61E the difference are more or less the same (~8-9 and ~4-5 respectively) for both ALA-X-ALA and GLY-X-GLY. These values mean however that the overall difference are more or less the same. Another promising candidate is the combination of a bigger box size and shifting ions, this one has much poorer values with ALA-X-ALA. The differences here are ~2.7 for T47E, ~82 for T53E, ~1 for S54E and ~9 for S61E. this means that in comparison to PME and shifting ions 3 of the 4 difference are smaller but one (T53E) is significantly larger. Using a bigger box size, PME and shifting ions does make the differences even smaller as under those conditions the difference between GROMOS and AMBER are ~30-40 kJ/mol for all residues except S61E which has a difference of 2.42 kJ/mol.

With a few exceptions the GLY-X-GLY values of the Martini force field were within 2.5 kJ/mol of their ALA-X-ALA counterparts. For the GROMOS force field the GLY-X-GLY values were within 2.5 kJ/mol of their ALA-X-ALA counterparts unless shifting ions are used. For the AMBER force field the GLY-X-GLY values differ by ~ 2.5 kJ/mol with ALA-X-ALA when a smaller box size without shifting ions is used but are more negative (≥ 10 kJ/mol) when a bigger box size or shifting ions are used.

The standard deviations are typically within or close to 2.5 kJ/mol for GROMOS and Martini and around the 5-8 kJ/mol (sometimes reaching 10 kJ/mol) for AMBER (figure S2). The standard deviations when using shifting ions are around the 6 kJ/mol for GROMOS, 10 kJ/mol for AMBER and within 2.5 kJ/mol for the Martini force field (sometimes reaching 5 kJ/mol) (figure S3). It must be noted however that for GROMOS and AMBER standard deviations as high as 15 kJ/mol could be reached.

Splitting the TI into two parts did significantly affect the final values (difference ~ 20 kJ/mol). Which means that splitting up the simulation can cause some unreliability in the results. On the other hand, the combination of ions that shift state and a bigger box size reduces the differences between the averages values to be smaller than 0.5 kJ/mol (for both ALA-X-ALA and GLY-X-GLY conditions), but the standard deviation under those conditions can be rather large so this needs to be interpreted with caution.

In depth description of the simulation of the phosphorylations

Phosphorylating the key residues (T47, T53, S54 and S61) (figure S4) gave $\Delta\Delta G$ s that are almost all negative indicating that the phosphorylation increased the free energy of folding and destabilizing the SNARE.

For the GROMOS simulations increasing the box size (figure S4) did significantly alter the $\Delta\Delta G$, especially in the case of S54pS which became ~ 50 kJ/mol more negative. Because the other $\Delta\Delta G$ s remain became ~ 20 - 30 kJ/mol less negative than those of the smaller box, the shift of S54pS altered the pattern of the relative effects of the residues. This holds true for both ALA-X-ALA and GLY-X-GLY.

In contrast to the mutations to GLU and ALA the Martini fc_100000 and fc_1000000 (figure S4) have the same pattern of relative effects and have very similar values (with the exception of T53E they are all within 2.5 kJ/mol of each other) in case of the ALA-X-ALA simulations. The pattern of relative effects are however different when comparing in the GLY-X-GLY. In case of the fc_100000 the T47pT and T53pT both have a higher $\Delta\Delta G$ than S54pS, while in case of the fc_1000000 both have a lower $\Delta\Delta G$. The values of S54pS and S61pS have a difference smaller than 2.5 kJ/mol between the fc_100000 and fc_1000000 variants. S61pS is positive in value although only slightly so (~ 2 kJ/mol).

For the GROMOS simulations using PME (figure S4) made T47pT less negative by about 5 kJ/mol, T53pT and S54pS more negative by ~ 25 kJ/mol and ~ 15 kJ/mol respectively and S62pS less negative by ~ 10 kJ/mol. For GLY-X-GLY (figure S4) the effects were somewhat different; T47pT became less negative by about 10 kJ/mol, T53pT and S54pS more negative by ~ 20 kJ/mol and ~ 15 kJ/mol respectively and S62pS less negative by ~ 12 kJ/mol. This alters the pattern again as T53pT will have a more negative value than T47E, which is the opposite of what is the case under conditions without alterations.

If a bigger box size and PME (figure S4) are used then T47pT, T53pT and S61pS become less negative by ~8, ~20 and ~30 kJ/mol respectively, while S54pS becomes more negative by ~7 kJ/mol; this holds true for both ALA-X-ALA and GLY-X-GLY. In comparison to when only a bigger box size is used T47pT and T53pT are more negative while S54pS and S61pS are less negative, but for the rest the pattern of relative effects is the same. In comparison to when only PME is used the pattern changes again as the $\Delta\Delta G$ of T53E becomes less negative than S54E, the resulting pattern matches that of the mutations to glutamate.

For Martini fc_100000 using PME (figure S4) makes T47pT, T53pT and S54pS more negative by ~25, ~10 and ~17 kJ/mol respectively; while S61pS remains within 2.5 kJ/mol of the original values. This holds true for both ALA-X-ALA and GLY-X-GLY (figure S4). For Martini fc_1000000 using PME makes T47pT, T53pT and S54pS more negative by ~20, ~5 and ~10 kJ/mol respectively for both ALA-X-ALA and GLY-X-GLY; while S61pS goes from 1.82 to -3.72 for ALA-X-ALA and from 2.48 to -1.66 for GLY-X-GLY. The patterns of relative expression already present for both ALA-X-ALA and GLY-X-GLY were not altered by the use of PME, nor did the values of the Martini force field closer to those of GROMOS. The difference between the $\Delta\Delta G$ s of fc_100000 and fc_1000000 also remained more or less the same, with the differences being within 5 kJ/mol of their values without PME.

For the GROMOS simulations using shifting ions (figure S4) makes T47pT, T53pT, S54pS and S61pS more negative by ~70, ~25, ~60 and ~20 kJ/mol respectively. This did however alter the pattern of relative expression as S54pS became more negative than T53pT which is the opposite of the situation under conditions without alterations, but the resulting pattern of relative effects is however similar to that of mutation to glutamate.

Increasing the box size in addition to using shifting ions (figure S4) makes the $\Delta\Delta G$ s less negative in comparison to when only shifting ions are used; T47pT, and T53pT become less negative by ~65 kJ/mol and ~38 kJ/mol, while S61pS becomes more negative by ~6 kJ/mol and S54pS even gains a positive value of 17.91 kJ/mol. It must be noted however that S54pS has a standard deviation of 23.08 kJ/mol which means the $\Delta\Delta G$ may also be in the negatives. The pattern of relative effects was also altered as prior to increasing the box size S54pS had a less negative value than T53pT while after the box size increased the roles were reversed. The resulting pattern is less optimal as the symmetry with the mutations to glutamate is broken and S54pS becomes positive which is unusual as mutations to glutamate are destabilizing and should thus give a negative $\Delta\Delta G$.

When using PME in combination with shifting ions (figure S4) all $\Delta\Delta G$ s become a lot less negative; T47pT, T53pT and S54pS become less negative by ~120, ~54 and ~24 kJ/mol respectively, S61pS becomes strongly positive becoming more positive by 105.80 kJ/mol ending up at a value of 43.87 kJ/mol. The standard deviation of S61pS is 16.93 kJ/mol but this is not enough to place the $\Delta\Delta G$ within the negatives. The pattern of relative effects alters again in comparison to when only shifting ions are used, now resembling the pattern found for mutations to glutamate.

Using a bigger box size and PME and shifting ions (figure S4) will alter the $\Delta\Delta G$ s in a mixed manner in comparison to when only PME and shifting ions are used. T47pT becomes more negative by ~10 kJ/mol, T53pT becomes less negative by ~4 kJ/mol, S54pS remains within 2.5 kJ/mol of the values of prior to increasing the box size, S61pS decreases to 0.29 kJ/mol. The standard deviation of S61pS remains more or less the same, which means that the $\Delta\Delta G$ can end up in the negative values. Here the pattern of relative effects remained the same as prior to increasing the box size, meaning that for

phosphorylation the pattern of relative effects will only stop changing when both PME and shifting ions are used.

For GLY-X-GLY (figure S4) the shifts in $\Delta\Delta G$ are somewhat different. The shifts between the use of shifting ions and conditions without alterations are more or less the same as with ALA-X-ALA for T47pT (~70 kJ/mol) and T53pT (~25 kJ/mol), for S54pS the shift is ~27 kJ/mol vs ~60 kJ/mol with ALA-X-ALA, for S61pS the shift is 14.49 kJ/mol vs the 18.18 kJ/mol of ALA-X-ALA, the shifts are however all in the same direction as with ALA-X-ALA. The shift induced by increasing the box size is the same as with ALA-X-ALA. However S54pS gains a positive value of 48.34 kJ/mol instead of 17.91 kJ/mol. The standard deviation of S54pS is 27.29 kJ/mol which is not enough to put the $\Delta\Delta G$ in the negatives. When using PME and shifting ions the shift in comparison to when only shifting ions are used is however different from that of ALA-X-ALA. The $\Delta\Delta G$ s of T47pT and T53pT became less negative by ~80 and ~15 kJ/mol respectively, while S54pS becomes more negative by ~26 kJ/mol and S61pS becomes more positive by 56.16 kJ/mol ending up at 24.66 kJ/mol. The standard deviation of 15.52 is not enough to place S61pS in the negatives. Again the effect of increasing the box size was the same as with ALA-X-ALA. The pattern of relative effect is the same as with ALA-X-ALA under all possible conditions even if the exact values can differ significantly.

When using shifting ions (figure S4) the $\Delta\Delta G$ s of Martini fc_100000 remained within or close to 2.5 kJ/mol of the values under conditions without alterations, the exception being T53pT where the $\Delta\Delta G$ from -2.99 to 2.19 kJ/mol. For GLY-X-GLY (figure S4) the shift is different as while S54pS and S61pS remained within or close to 2.5 kJ/mol of the values under conditions without alterations, T47pT became less negative by ~15 kJ/mol while T53pT went from -4.32 to 16.17 kJ/mol. The standard deviation of T53pT is 2.45 which is not large enough to make the $\Delta\Delta G$ end up in the negatives. For Martini fc_1000000 again the $\Delta\Delta G$ s shifted more strongly than for the fc_100000 variant; T47pT and S54pS became less negative by ~5 kJ/mol, T53pT remained within 2.5 kJ/mol of the values under conditions without alterations, while S61pS became more positive by ~6 kJ/mol. Again for GLY-X-GLY the shift is different; T47pT and T53pT became less negative by ~5-6 kJ/mol, S54pS remained close to 2.5 kJ/mol of the values under conditions without alterations and S61pS became more positive by ~6 kJ/mol.

For ALA-X-ALA the $\Delta\Delta G$ s of fc_100000 and fc_1000000 were more deviant from each other than under conditions without alterations, but with the exception of T53pT all values were within 5.0 kJ of their counterparts. Just as before this not the case with GLY-X-GLY where there is a difference of ~20 and ~35 kJ/mol between fc_100000 and fc_1000000 for T47pT and T53pT respectively. S61pS is only 3 kJ/mol higher than for fc_1000000 than for fc_100000 and with S54pS the difference is smaller than 0.5 kJ/mol. For both ALA-X-ALA and GLY-X-GLY the patterns of relative expression are the same as under conditions without alterations. The difference in $\Delta\Delta G$ values between GROMOS and Martini are overall not smaller than under conditions without alterations.

For Martini fc_100000 using PME in combination with shifting ions (figure S4) makes T47pT more negative by ~25 kJ/mol, T53pT go from 2.19 to -15.62 and S54pS and S61pS remain close to 2.5 kJ/mol of their values when only shifting ions are used. For GLY-X-GLY (figure S4) the shift was different; T47pT and S54pS became more negative by ~35 and ~5 kJ/mol respectively, T53pT went from 16.17 to -11.41 kJ/mol, S61pS decrease by ~4 kJ/mol. The $\Delta\Delta G$ s of T47pT and T53pT are within

5 kJ/mol of their ALA-X-ALA counterpart, while S54pS and S61pS are within 0.5 kJ/mol of their ALA-X-ALA counterpart. This indicates a decent match between the values of ALA-X-ALA and GLY-X-GLY.

For Martini $fc_{1000000}$ T47pT became more negative by ~ 20 kJ/mol, Both T53pT and S54pS became more negative by ~ 5 kJ/mol and S61pS decreased by ~ 4 kJ/mol. For GLY-X-GLY the shift was the same. The $\Delta\Delta G$ values of T47pT and T53pT are ~ 14 kJ/mol more negative than their ALA-X-ALA counterparts, while S54pS and S61pS are within 1 kJ/mol of their ALA-X-ALA counterparts. This does however mean that here the overlap is worse between ALA-X-ALA and GLY-X-GLY than for the lower force constant.

For ALA-X-ALA the $\Delta\Delta G$ of T47pT $fc_{1000000}$ was ~ 9 kJ/mol more negative than its fc_{100000} counterpart, T53pT, S54pS and S61pS were all within or close to 2.5 kJ/mol of their fc_{100000} counterparts. For GLY-X-GLY T47pT and T53pT $fc_{1000000}$ are respectively ~ 10 and ~ 15 kJ/mol more negative than their fc_{100000} counterparts. For the $fc_{1000000}$ the $\Delta\Delta G$ s are with the exception of S54pS all within 8 kJ/mol of their counterparts in GROMOS with a bigger box size, PME and shifting ions. In case of T53pT and S61pS the difference are within or close to 2.5 kJ/mol. While again with the exceptions of S54pS this even lower with fc_{100000} that only holds true for ALA-X-ALA. For GLY-X-GLY the differences are larger than for ALA-X-ALA; with fc_{100000} 33.38, 40.74, 77.21 and 20.53 kJ/mol for T47pT, T53pT, S54pS and S61pS respectively, with $fc_{1000000}$ 5.15, 19.74, 72.83 and 24.60 for T47pT, T53pT, S54pS and S61pS respectively.

The standard deviations are around kJ/mol for both GROMOS and Martini force field (figure S4), except for Martini fc_{100000} without PME where the standard deviations are smaller than 2.5 kJ/mol. The standard deviations when using shifting ions are typically around the 10-15 (sometimes as high as 20) kJ/mol for GROMOS. For the Martini force field the standard deviations are within or close to 2.5 kJ/mol when shifting ions are used but not PME, when both shifting ions and PME are used the standard deviations are around the 5 kJ/mol for threonine phosphorylation but within 2.5 kJ/mol for serine phosphorylation.

References:

1. Malmersjö, S. *et al.* Phosphorylation of residues inside the SNARE complex suppresses secretory vesicle fusion. *EMBO J.* **35**, 1810–1821 (2016).